Electronic Supplementary Material (ESI) for Inorganic Chemistry Frontiers.
This journal is © the Partner Organisations 2023

Supplementary material

1. The schematic diagram of the commercial ceramic chip and the heater temperature and power vs. applied voltage curves; The schematic diagram of testing system for gas sensing.
2. SEM images of the samples: (a) S1, (b) S2, (c) S4 and (d) S5 at 50k.
3. Calculation process of the grain size.
4. Grain sizes and error bars of samples S1 – S5.
5. N_2 adsorption isotherms and BET surface area of the S2, S4 and S5 samples.
6. Pore size distributions of samples S1 – S5.
7. Response and recovery curves of (a) S1; and (b) S3 to 200 ppm H_2 at 150 °C; (c) S1 to 200 ppm H_2 at 250 °C.
8. Response curves in stability of S1 and S3 sensors.
9. Theoretical limit of detection (LOD).
10. Current vs. Voltage behaviors of S1 and S3 sensors at 150 ℃.
11. SEM images of the samples: (a) S1 and (b) S3 at 5k; (c) S3 at 50k.
12. Comparison of H_2 sensors based on different materials.

High-response H_2 sensing performances of ZnO nanosheets modulated by oxygen vacancies

Shiyu Zhou,[a] Wenjun Yan,*[a,b] Min Ling*[a,c] and Chengdu Liang*[a,c]

[a] *College of Chemical and Biological Engineering, Zhejiang University, Hangzhou 310027, China*

[b] *School of Automation, Hangzhou Dianzi University, Hangzhou 310018, China*

[c] *Institute of Zhejiang University-Quzhou, 78 Jiuhua Boulevard North, Quzhou 324000, China*

**Corresponding author:* yanwenjun@hdu.edu.cn; minling@zju.edu.cn; cdliang@zju.edu.cn

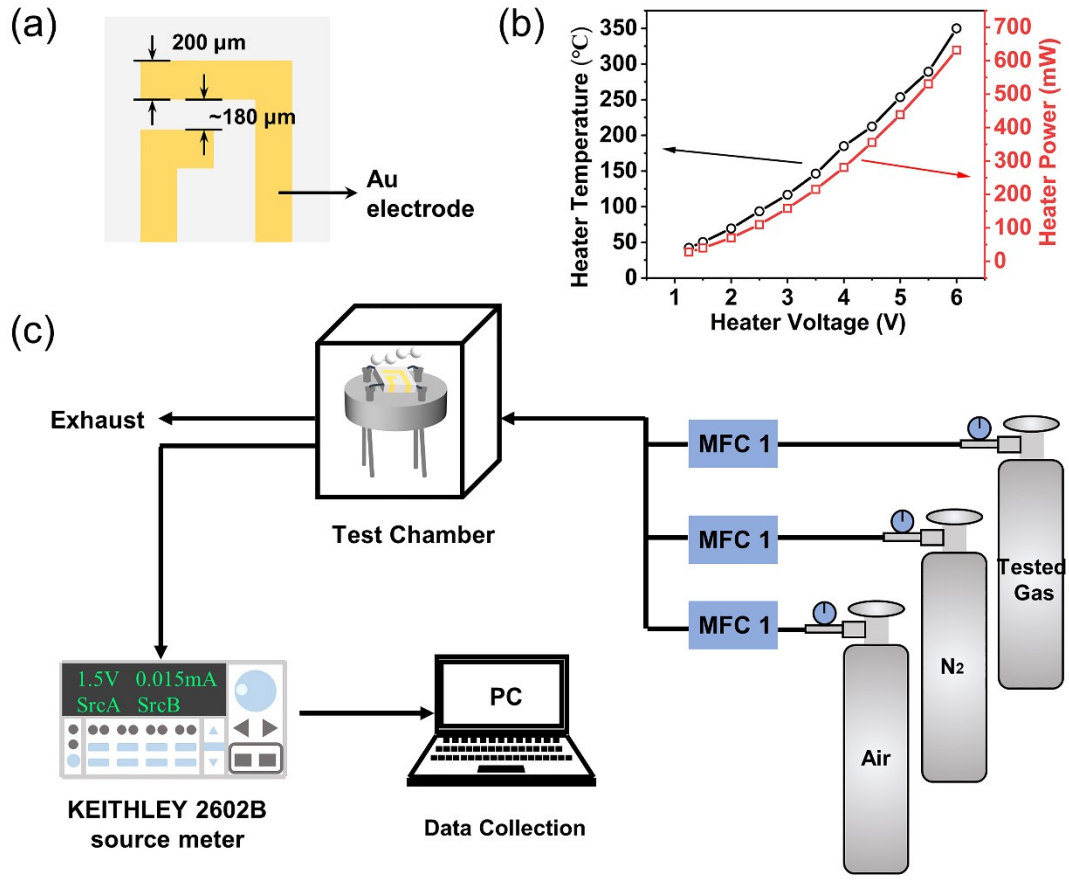

Fig. S1 (a) The schematic diagram of the commercial ceramic chip; (b) The heater temperature and power vs. applied voltage curves; (c) The schematic diagram of testing system for gas sensing.

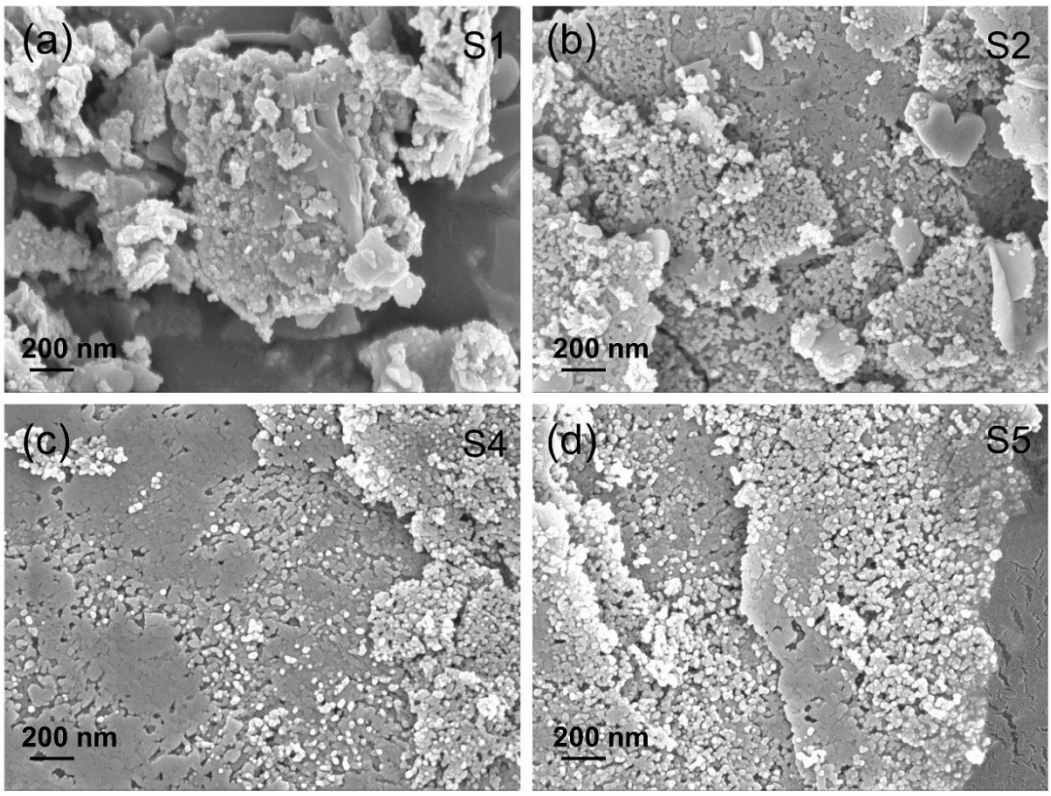

Fig. S2 SEM images of the samples: (a) S1, (b) S2, (c) S4 and (d) S5 at 50k.

Calculation process of the grain size.

The grain size is calculated according to the XRD results and Scherrer's equation:

$$D = \frac{K\lambda}{\beta cos\theta} \quad \text{(eqn S1)}$$

where D is grain size, K is Scherrer constant (0.89), λ is CuKα wavelength (1.54056 Å), β is peak width at half-height (FWHM), and θ is diffraction angle.

Here, we chose three main peaks ((100), (002), and (101)) to calculate the average grain size.

Table. S1 Grain sizes and error bars of samples S1 – S5.

Samples	Grain size (nm)	error bar (nm)
S1	16.58	4.11
S2	16.56	2.78
S3	15.99	2.79
S4	17.66	2.78
S5	15.64	3.17

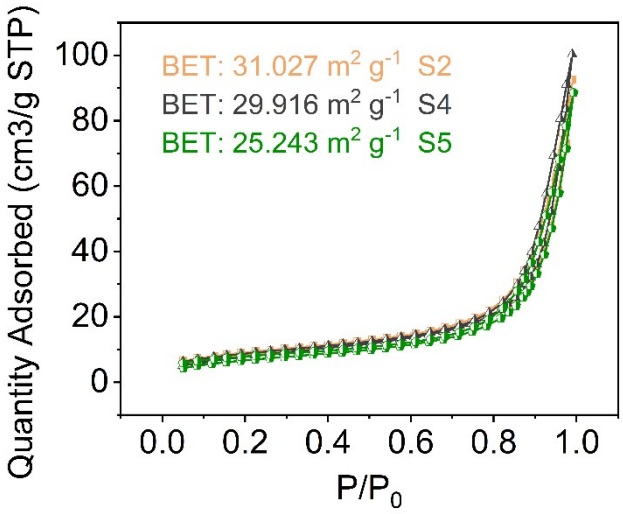

Fig. S3 N_2 adsorption isotherms and BET surface area of the S2, S4 and S5 samples.

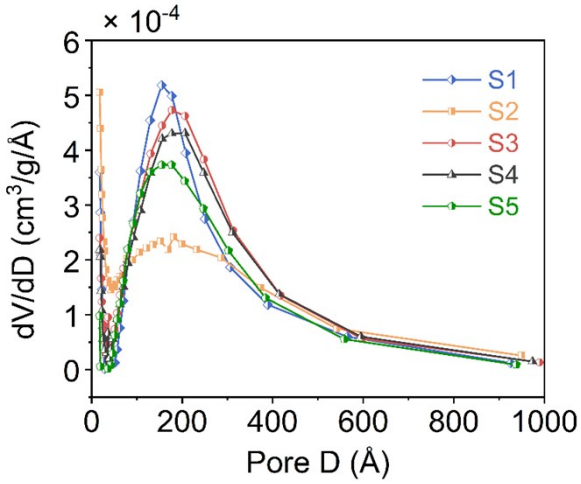

Fig. S4 Pore size distributions of samples S1 – S5.

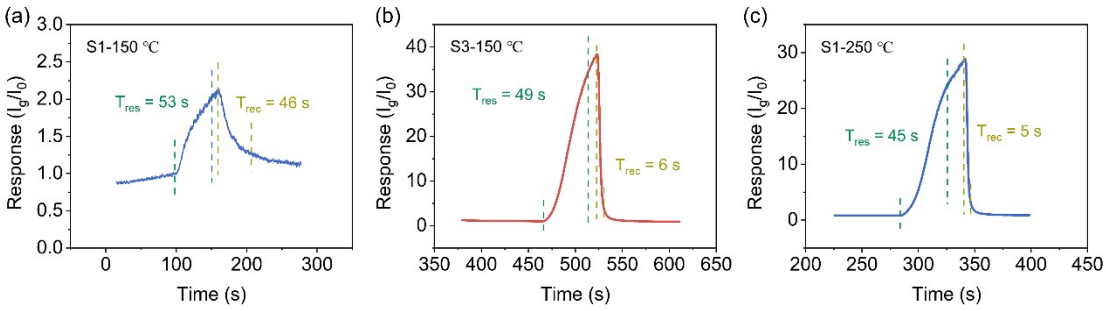

Fig. S5 Response and recovery curves of (a) S1; and (b) S3 to 200 ppm H_2 at 150 °C; (c) S1 to 200 ppm H_2 at 250 °C.

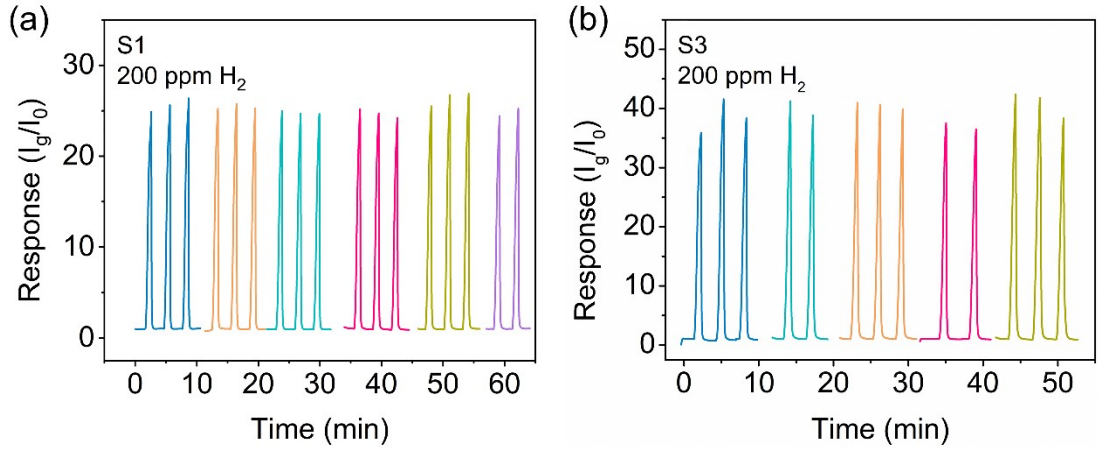

Fig. S6 Response curves in stability of S1 and S3 sensors.

Theoretical limit of detection (LOD).

According to the IUPAC (International Union of Pure and Applied Chemistry) definition, the signal could be considered as a true signal when the signal-to-noise ratio equals 3 [1]. Mathematically, the LOD could be calculated using the following equation

$$LOD = 3\frac{N_{rms}}{slope} \quad \text{(eqn S2)}$$

where N_{rms} is the root Mean square (RMS) noise formula, and slope is extrapolated from the linear calibration curve as shown in Fig. 5c. The limit of detection here is calculated to be 55 ppb."

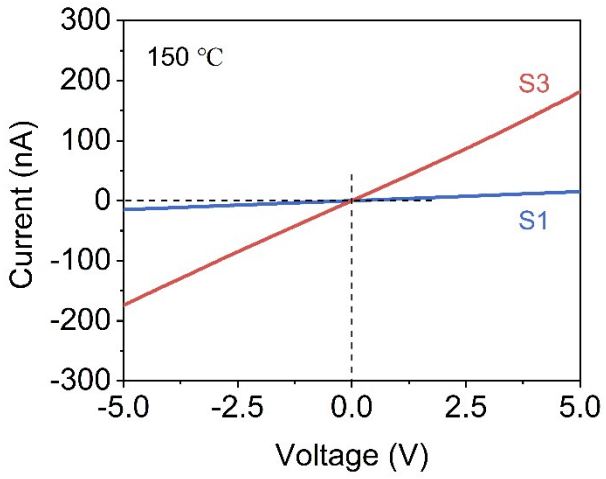

Fig. S7 Current vs. Voltage behaviors of S1 and S3 sensors at 150 ℃.

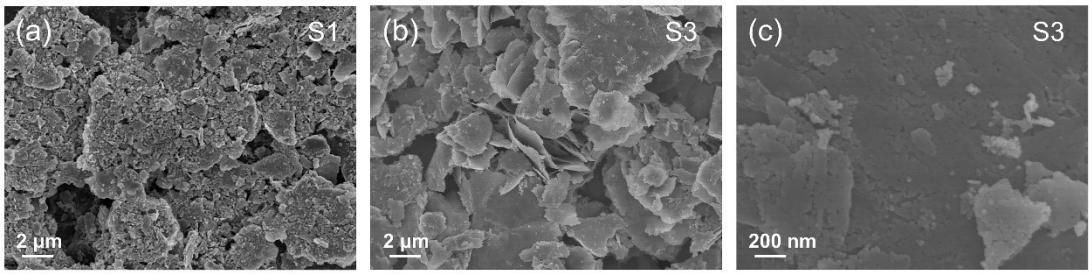

Fig. S8 SEM images of the samples: (a) S1 and (b) S3 at 5k; (c) S3 at 50k.

Table. S2 Comparison of H_2 sensors based on different materials.

No.	Materials	Temp. (℃)	R	LOD (ppm)	T_{rec} (s)	Ref.
1	ZnO with defects	150	38.2	0.055	6	This work
2	SnO_2 with defect	250	2.21	0.1	12	[S2]
3	ZnO/rGO composite	400	18	0.06	7	[S3]
4	Pd-decorated ZnO nanosheet	250	2.5	0.1	290	[S4]
5	Pd-ZnO nanoflowers	RT	1.7	0.01	165	[S5]
6	ZnO	190	1.25	0.01	960	[S6]
7	ZnO@400 sensor	RT	2.15	5	6	[S7]
8	Pd@ZnO-In_2O_3	350	42	5	240	[S8]

References

1. L. A. Currie, Nomenclature in evaluation of analytical methods including detection and quantification capabilities (IUPAC Recommendations 1995), *Pure and Applied Chemistry*, 1995, **67**, 1699-1723.
2. N. Luo, C. Wang, D. Zhang, M. Guo, X. Wang, Z. Cheng and J. Xu, Ultralow detection limit MEMS hydrogen sensor based on SnO_2 with oxygen vacancies, *Sens. Actuators, B*, 2022, **354**, 130982.
3. S. Zhou, J. Ji, T. Qiu, L. Wang, W. Ni, S. Li, W. Yan, M. Ling and C. Liang, Boosting selective H_2 sensing of ZnO derived from ZIF-8 by rGO functionalization,

Inorg. Chem. Front., 2022, **9**, 599-606.

4. J.-H. Kim, A. Mirzaei, M. Osada, H. W. Kim and S. S. Kim, Hydrogen sensing characteristics of Pd-decorated ultrathin ZnO nanosheets, *Sens. Actuators, B*, 2021, **329**, 129222.
5. J. Y. Jeon, S. J. Park and T. J. Ha, Functionalization of Zinc Oxide Nanoflowers with Palladium Nanoparticles via Microwave Absorption for Room Temperature-Operating Hydrogen Gas Sensors in the ppb Level, *ACS Appl. Mater. Interfaces*, 2021, **13**, 25082-25091.
6. Ö. Barin, A. Ajjaq, A. O. Çağırtekin, I. Karaduman Er, M. A. Yıldırım, A. Ateş and S. Acar, Pivotal role of nucleation layers in the hydrothermally-assisted growth of ZnO and its H_2 gas sensing performance, *Sens. Actuators, B*, 2022, **371**, 132499.
7. M. Kumar, V. Bhatt, J. Kim, A. C. Abhyankar, H.-J. Chung, K. Singh, Y. B. Cho, Y. J. Yun, K. S. Lim and J.-H. Yun, Holey engineered 2D ZnO-nanosheets architecture for supersensitive ppm level H_2 gas detection at room temperature, *Sens. Actuators, B*, 2021, **326**, 128839.
8. T. T. D. Nguyen, D. Van Dao, I.-H. Lee, Y.-T. Yu and S.-Y. Oh, High response and selectivity toward hydrogen gas detection by In_2O_3 doped Pd@ZnO core-shell nanoparticles, *J. Alloys Compd.*, 2021, **854**, 157280.